MAP551 - PC7 - Spatially extended systems of equation Equilibria, traveling waves and Turing patterns.

Paul Calot

November 30, 2020

0.1 Introduction

0.2 Thermal explosion - 1D problem

0.2.1 Link with 0D problem studied in the PC1

0.2.1.1

In the following, we supposed that the conditions to exchange $\int_a^b f(z)dz$ and the derivative along t are met.

Integrating equation (1) yields :

$$\frac{d\bar{Y}}{dt} - \frac{D}{2L}\int_0^{2L} \partial_{zz}Y(t,z)dz = \frac{-B}{2L}\int_0^{2L} e^{\frac{-E}{RT}}Ydz$$

With : $\int_0^{2L} \partial_{zz}Y(t,z)dz = \frac{D}{2L}(\partial_z(t,2L) - \partial_z Y(t,0)) = 0$ using the Neumann boundary condition.

Which yields :

$$\frac{d\bar{Y}}{dt} = -\frac{B}{2L}\int_0^{2L} e^{\frac{-E}{RT}}Ydz$$

Integrating equation (2) yields :

$$\partial_t\bar{T} = \frac{D}{2L}\int_0^{2L} \partial_{zz}Tdz + (T_b - T_0)\frac{B}{2L}\int_0^{2L} e^{-\frac{E}{RT}}Ydz$$

.

0.2.1.2

Inequality on $\bar{Y}$ and convergence : By hypothesis, we have $T(t,z) \geq T_0 \Rightarrow e^{\frac{-E}{RT_0}} \leq e^{\frac{-E}{RT(t,z)}}$ which in turn yields :

$$d_t\bar{Y} \leq \frac{-B}{2L}e^{\frac{-E}{RT_0}}\int_0^{2L} Ydz = -\alpha\bar{Y}$$

With $\alpha = Be^{\frac{-E}{RT_0}}$.

Thus :

$d_t\bar{Y} + \alpha\bar{Y} \leq 0 \Rightarrow (e^{\alpha t}\bar{Y}) \leq 0 \Rightarrow e^{\alpha t}\bar{Y}(t) \leq \bar{Y}(0)$

Which yields :

$$\bar{Y}(t) \leq (e^{-\alpha t}\bar{Y}(0)$$

Which converge towards 0 in an exponential manner.

This spatial-average behavior is consistant with what we saw in *PC1*.

Inequality on $\bar{T}$ and convergence : From previous question and the convergence of $\bar{Y}$, we have :

$0 \leq (T_b - T_0)\frac{B}{2L}\int_0^{2L} e^{-\frac{E}{RT}}Ydz \leq \alpha(T_b - T_0)\bar{Y}(t) \to 0.$

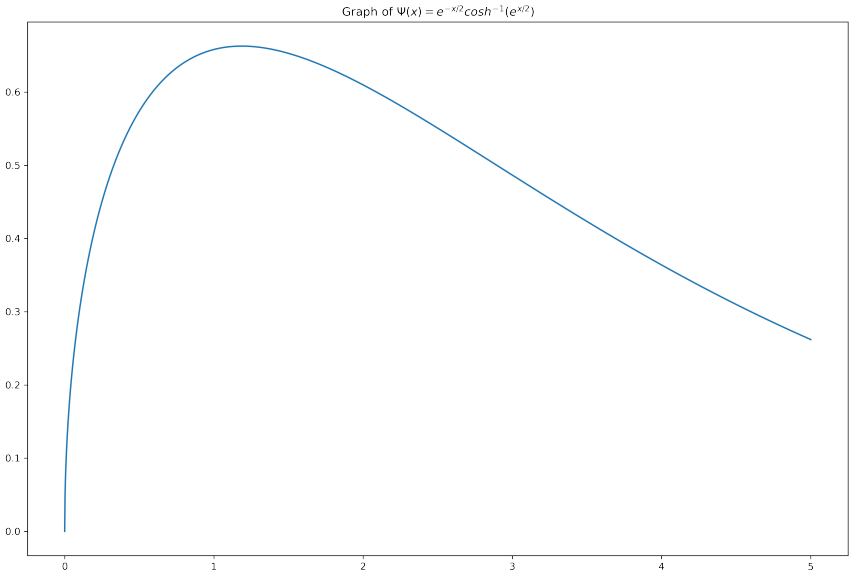

Figure 1: Graph of $\Psi(x) = e^{-x/2}cosh^{-1}(e^{x/2})$. The maximum is roughly 0.66 which means: $\lambda_{cr} \approx 0.87$.

0.2.1.3

The space-averaged asymptotic values are:

1. For $\bar{Y}$, the decrease is exponential, and converged towards 0. This is consistant with PC1.
2. For $\bar{T}$, the average converges towards T_0. For the homogeneous system in PC1, getting the same limit behavior required taking in account thermal loss by adding a term proportionnal to $T_0 - T$ to $(T_b - T_0)Be^{-\frac{E}{RT}}Y$. Not taking it into account showed the temperature only go up and converge towards T_b.

0.2.2 Stationary solution as equilibria of the infinite dimensional dynamical system - qualitative analysis

0.2.2.1 BONUS

0.2.2.2

The function Ψ is plotted in figure 0.2.2.2. It is differientable for all $x\ in \mathbb{R}_{+,*}$.

We see that :

$$\begin{cases} \Psi(x) \geq 0, \forall x \in \mathbb{R}_{+,*} \\ \Psi(x) \xrightarrow[x \to 0]{} cosh^{-1}(1) = 0 \\ \Psi(x) \xrightarrow[x \to +\infty]{} = 0 \end{cases} \tag{1}$$

Thus, the function Ψ being continuous, it is bounded above by Ψ^{max} which it necessarily reaches. Consequently and using the previous question, there is a critical parameter such that $\sqrt{\frac{\lambda_{cr}}{2}} = \Psi^{max}$.

There is thus three possibilities :

1. $\lambda < \lambda_{cr}$: then there is multiple solutions to the relation that must be satisfied by λ and θ_m^{st}. There exists multiple smooth, concave and symmetric stationary temperature profiles.
2. $\lambda = \lambda_{cr}$: only one smooth, concave and symmetric stationary temperature profile exists.
3. $\lambda > \lambda_{cr}$: no smooth, concave and symmetric stationary temperature profile exists.

0.2.2.3

For $\lambda < \lambda_{cr}$, graph 0.2.2.2 shows that there seems to be two solutions. Referring to the previous PC, it is likely that the first solution for which Ψ increases is unstable (the eigen value of the system is positive) and the second one is stable (Ψ decreases).

0.2.3 Numerical resolution of the semi-discretized in space problem

0.2.3.1

Semi-discretizing (3)-(4) and purely (5) yields :

$$\begin{cases} \partial_\tau \theta_k - \frac{1}{\lambda} \frac{\theta_{k+1}+\theta_{k-1}-\theta_k}{d\zeta^2} = exp(\theta_k) Y_k \ (3') \\ \partial_\tau Y_k - \frac{1}{\lambda} \frac{Y_{k+1}+Y_{k-1}-Y_k}{d\zeta^2} = -\epsilon exp(\theta_k) Y_k \ (4') \\ \frac{Y_{n+1,k}-Y_{n,k}}{dt} - \frac{1}{\lambda} \frac{Y_{n,k+1}+Y_{n,k-1}-Y_{n,k}}{d\zeta^2} = exp(\theta_k) \ (5') \end{cases}$$

Where : $X_{n+\alpha,k+\beta} = X(\tau + \alpha * d\tau, \zeta + \beta * d\zeta)$ (purely discretized) and $X_{k+\beta} = X(t, \zeta + \beta * d\zeta)$ (semi-discretized) with $k, n \in [0, K] \times [0, N]$ if the space is splitted into $K+1$ parts and if we consider $N+1$ time steps.

The semi-discretized system :

$$\begin{cases} \partial_\tau \theta_k - \frac{1}{\lambda} \frac{\theta_{k+1}+\theta_{k-1}-\theta_k}{d\zeta^2} = exp(\theta_k) Y_k \\ \partial_\tau Y_k - \frac{1}{\lambda} \frac{Y_{k+1}+Y_{k-1}-Y_k}{d\zeta^2} = -\epsilon exp(\theta_k) Y_k \end{cases}$$

can be viewed as a non linear, first-order ordinary differential equation : $X'(t) = f(t, X(t), \Lambda)$ with $\Lambda = (\lambda, \epsilon, d\zeta)$.

0.2.3.2

0.3 Study of Combustion waves

The system numerical solution for $\lambda = 0.5$ is given in figure 2. The system needs time to converge and thus increasing the integration time was required. The convergence of the system means that $\lambda < \lambda_{cr}$ for which there are two solutions. In order to guess which one is stable, we can lower λ and see what happens for θ_{max} : if it goes down, then the left solution is stable, else the right is stable. The solution is consistant with the analytical one we got and the hypotheses we made : the stationary temperature profiles are smooth, concave and symmetric.

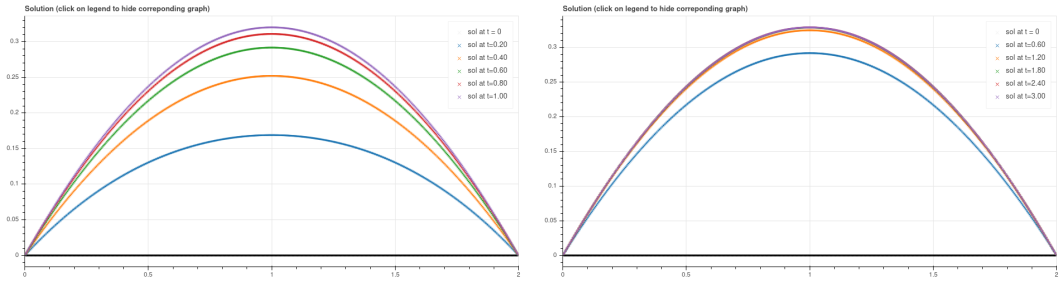

Figure 2: Integration with Radau5 (which is much better than Rock4) of the system for $\lambda = 0.5$ and different integration time (from left to right) : 1 second, 3 seconds.

On graph 3 are plotted two solutions for $\lambda = 0.5$ (left) and 0.3 (right). We see that lowering λ causes the max temperature to be lowered too. Thus, the left solution (see graph 0.2.2.2) is the sable one.

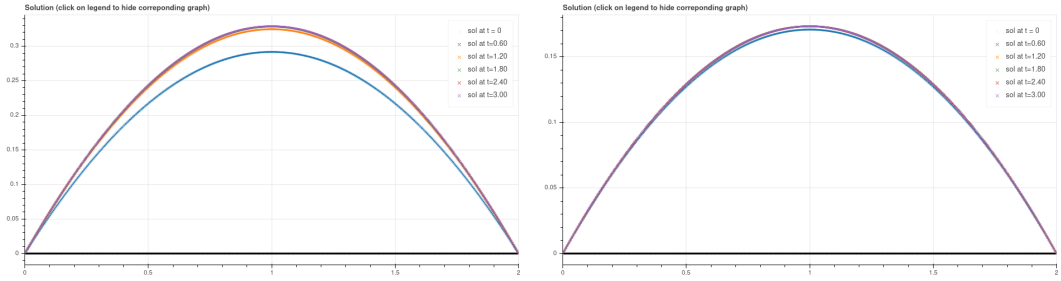

Figure 3: Integration with Radau5 of the system for $\lambda = 0.5$ (left) and $\lambda = 0.3$ (right). The left solution on graph 0.2.2.2 is the stable one.

Graph 4 shows that $\lambda_{cr} \approx 0.87 - 0.88$ as the system seems to lose it concavity for such values. There may still exists solutions but they would not be smooth, concave and symmetric.

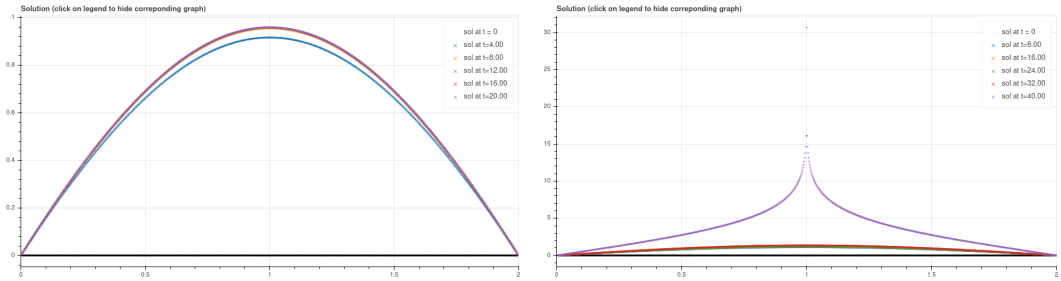

Figure 4: Integration with Radau5 of the system for $\lambda = 0.86$ (left) and $\lambda = 0.88$ (right). The right solution does not verify the hypotheses and thus can tell us that $\lambda_{cr} \approx 0.88$.

0.3.0.1

Graph 5 shows the mass fraction solution of the system converging quickly towards $Y \equiv 1$.

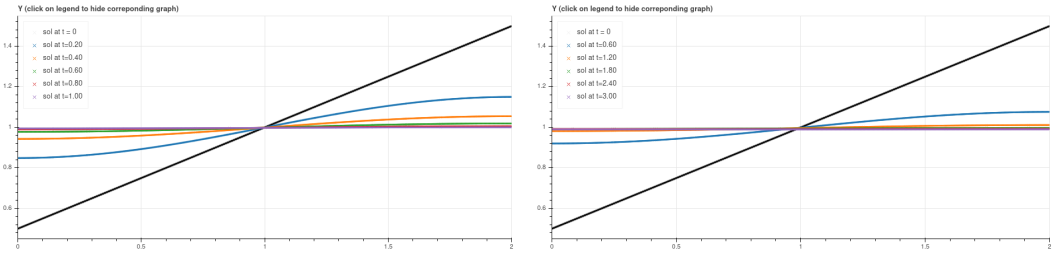

Figure 5: Integration of the system for $\lambda = 0.5$ (left) and $\lambda = 0.9$. We see that the diffusion for $\lambda = 0.5$ takes less that one second. We also see that the closer we get from a homogenize system, the slower the diffusion gets, which makes perfect sense since the concentration gradients are lower.

0.3.0.2

We explored in this PC the influence of taking into account an inhomogeneous space distribution initially and broadly speaking a space-dependent system.

Several remarks can be made :

1. The space average asymptotic values of temperature and mass fraction for the space-dependent system are close to the second simplified model of PC1. Y is converging toward 0 while the temparature which starts by increasing finally decreases to T_0.

2. In PC1 last model with convection taking into account, we saw that when the convection was too important, the system could explode in temperature. We have a similar behavior here with the diffusion being too quick : when λ is above a certain critical value, then there is no more a smooth, symmetric and concave profile and graph 4 right figure suggests it may even be exploding.

3. When λ is below the critical value, then stable temperature and mass fraction profiles are quicky reachy (several seconds) as graph 5 displays for the mass fraction (see graph 2 for example for the temperature profile).

0.3.1 Travelling waves

0.3.1.1

Using : $Y(t,x) = \Phi(y)$ and $\Theta(t,x) = \theta(y)$ with $y = x - ct$, we have :

$$\begin{cases} \partial_t Y &= -c\Phi'(y) \\ \partial_t \Theta &= -c\theta'(y) \\ \partial_{xx} Y &= \Phi''(y) \\ \partial_{xx} \Theta &= \theta''(y) \end{cases}$$

Which yields:

$$(6) \Leftrightarrow \begin{cases} -c\Phi' - D\Phi'' = -\tilde{\psi}(\theta)\Phi \\ -c\theta' - D\theta'' = \tilde{\psi}(\theta)\Phi \end{cases} \qquad \text{(eq 3.1.1)}$$

0.3.1.2

Using (eq 3.1.1) and summing the two *ODE*, we have :

$$-c\mathcal{H}' - D\mathcal{H}'' = 0$$

Which yields: $\mathcal{H}'(y) = Ke^{\frac{c}{D}y}$, $K \in \mathbb{R}$.

However, the conditions at infinity are : $\mathcal{H}(y) \xrightarrow[y\to\pm\infty]{} 1$. Consequently, $\mathcal{H}$ being a differentiable function on $\mathbb{R}$, an adapted version of Rolle's theorem (we can show that with these conditions at infinity, there necessarily is a maximum or minimum for H in $\mathbb{R}$) applies and we have : $\exists a \in \mathbb{R}, \mathcal{H}'(a) = 0$.

This yields : $\forall y \in \mathbb{R}, \mathcal{H}'(y) = 0$.

Which finally yields using the limits in $\pm\infty$:

$$\forall y \in \mathbb{R}, \mathcal{H}(y) = cte = 1.$$

0.3.1.3

From the previous question, we can write :

$$\begin{cases} \Phi & = 1 - \theta \\ c\theta' + D\theta'' & = -\psi(\theta) \end{cases}$$

with : $\psi(\theta) = \tilde{\psi}(\theta)(1-\theta)$.

Which requires only to solve $c\theta' + D\theta'' + \psi(\theta) = 0$ (equation (7)) to solve the problem.

0.3.1.4

We proceed in two phases.

First, show that the function is decreasing :

Suppose that : $\exists y, \theta(y) > 0$.

Then, using the limits at infinity, we can find y_1 and y_2 such that : $y_1 \leq y \leq y_2$ and $\theta'(y_1) = \theta'(y_2) = 0$.

On this interval, $\psi > 0$ and $\theta' > 0$ thus $\theta'' < 0$. This means θ is a concave function on this interval which contradicts the hypothesis that $\theta'(y) > 0$.

Consequently, θ is non-increasing.

Second, show that the function is stricly decreasing :

Suppose that : $\exists y_0, \theta'(y_0) = 0$.

Thus (7) yields : $D\theta''(y_0) + \phi(\theta(y_0)) = 0$ with $\phi(\theta(y_0)) \geq 0$.

There are two cases :

1. If $\phi(\theta(y_0)) > 0$, then $\theta''(y_0) < 0$ thus $\theta'({y_0}^-) > 0$ which contradicts the first point.
2. Else ($\phi(\theta(y_0)) = 0$), then $\theta''(y_0) = 0$. However, Cauchy-Lipschitz theorem applies for (7) and there is a unique solution for the initial conditions :

$$\begin{cases} \theta(y_0) & = \theta_0 \\ \theta'(y_0) & = 0 \end{cases}.$$

Which yields : $\theta(y) = \theta_0, \forall y$. This contradicts the conditions at infinity.

Thus, for the conditions at infinity and (7), θ is necessarily strictly decreasing.

0.3.1.5

Using : $\tilde{p} = -\theta'$, (7) becomes:

$$(7) \Leftrightarrow \begin{cases} \tilde{p} & = -\theta' \\ D\tilde{p'} & = -c\tilde{p} + \psi(\theta) \end{cases} \tag{3.1.5}$$

Which is a system of first order ODEs.

0.3.1.6

Using :

$$\begin{cases} s & = \theta(y) \\ p(s) & = \tilde{p}(y) \end{cases},$$

which yields $\tilde{p}'(y) = \theta'(y)p'(s) = -\tilde{p}(y)p'(s) = -p(s)p'(s)$, in the second equation of system 3.1.5, we have :

$$Dp(s)p'(s) = cp(s) - \psi(s).$$

In addition :

$$\begin{cases} p(0) & = \lim_{y\to+\infty} -\theta'(y) \\ p(1) & = \lim_{y\to-\infty} -\theta'(y) \end{cases} \Rightarrow \begin{cases} p(0) & = 0 \\ p(1) & = 0 \end{cases}.$$

Note that the equations is of first order and that we have two initial conditions. Consequently, the system does not necessarily have a solution (depending on c).

0.3.1.7

The system to be solved is ($D = 1$):

$$\begin{cases} pp' & = cp - \psi, \, [0,1] \\ p(0) & = 0 \\ p(1) & = 0 \end{cases} \tag{3.1.7}$$

The Taylor expansion of p close to 1 yields :

$$\begin{cases} p(s) = p(1) + p'(1)(s-1) + o(s-1) \\ \psi(s) = \psi(1) + \psi'(1)(s-1) + o(s-1) \end{cases} \Leftrightarrow \begin{cases} p(s) = \alpha(s-1) + o(s-1) \\ \psi(s) = -\gamma(s-1) + o(s-1) \end{cases}$$

Which using the ODE in system 3.1.7 yields to : $\alpha^2(s-1) + o(s-1) = c\alpha(s-1) + \gamma(s-1) + o(s-1)$ which, keeping only first order terms, yields : $\alpha^2 = c\alpha + \gamma$.

Thus :

$$\alpha = \frac{c \pm \sqrt{c^2 + 4\gamma}}{2}$$

Since $\gamma > 0$, there is a positive and a negative solution. However, p is decreasing close to 1, thus the negative solution is choosen.

This yields :

$$p'(1) = \alpha = \frac{c - \sqrt{c^2 + 4\gamma}}{2}.$$

0.3.1.8

Solution on $[\eta, 1]$

Focusing on $[\eta, 1]$, the ODE is : $pp' = cp - \psi$.

Which can be written : $\frac{1}{2}(p^2)' = cp - \psi$.

Or, with $u = p^2$, $\frac{1}{2}u' = c\sqrt{u} - \psi$.

Peano's theorem gives the existence of a solution on $[\eta, 1[$ of this equation. We need $u > 0$ to have the unicity which is the case when considering every $[\eta, s_2]$, $\eta \neq s_2 < 1$ (from 0.3.1.4 p is strictly positive on $]0, 1[$ and so is u).

Decreasing function of c **?**

We have : $\frac{d\alpha}{dc} = \frac{1}{2}(1 - \frac{c}{\sqrt{c^2+4\gamma}} > 0$.

Thus, if c increases, $\alpha = p'(1)$ increases (while being negative).

Thus, "close" to 1, $c_1 < c_2 \Rightarrow p_1 > p_2$. Call $\tilde{s}$ such that : $\forall s \geq \tilde{s}, p_1(s) > p_2(s)$. The solution being unique on $[\eta, \tilde{s}]$, p_1 and p_2 can never cross (and be equal at a given point) since $p_1(\tilde{s}) > p_2(\tilde{s})$.

Consequently, the solution p is a decreasing function of c.

Case $c = 0$ **:**

In this case, $u' = -2\psi$, which yields :

$$\int_\eta^1 u'(s)ds = -2\int_\eta^1 \psi(s)ds = -2\int_0^1 \psi(s)ds = -2I$$

Which yields : $u(\eta) - 0 = 2I$

Thus with $p \geq 0$: $p(\eta) = \bar{p} = \sqrt{2I}$.

This is the top envelop of the possible solutions (since we took $c = 0$ at its minimum value).

0.3.1.9

Solving on $[0, \eta[$ yields : $p' = c$ thus : $p(s) = cs + p(0) = cs$.

To have a solution, a necessary condition is : $c\eta = p_{sol, s\in[\eta,1[}(\eta)$. Note that, since $f : (t, p, c) \to 2(c\sqrt{p} - \psi)$ is differentiable on $]\eta, 1[$, the solution on $[\eta, 1[$ varies continuously with c.

We also note that the solution on $[0, \eta[$ increases with c increasing starting from $p = 0$ for $c = 0$ and that the solution on $[\eta, 1[$ decreases **continuously** with c increasing starting from $p = \sqrt{2I} > 0$.

Consequently, there is a c_0 such that there exist a continuous integral curve in the phase plane joining (0,0) and (1,0).

0.3.2 BONUS: Flame speed and its limit

0.4 Simulation of traveling waves: Nagumo

0.4.1

The stiffness of a system is relative to $|\lambda_{min}T|$ where T is the integration time and λ_{max} is the most negative eigen value. The maximum gradient norm is proportionnal to $(\frac{k}{D})^{\frac{1}{2}}$ which means that the bigger it is, the smaller λ_{min} is and thus the stiffer the system (at fixed T).

Graph 6 shows two simulations with different values of gradient but same value for the speed of propagation.

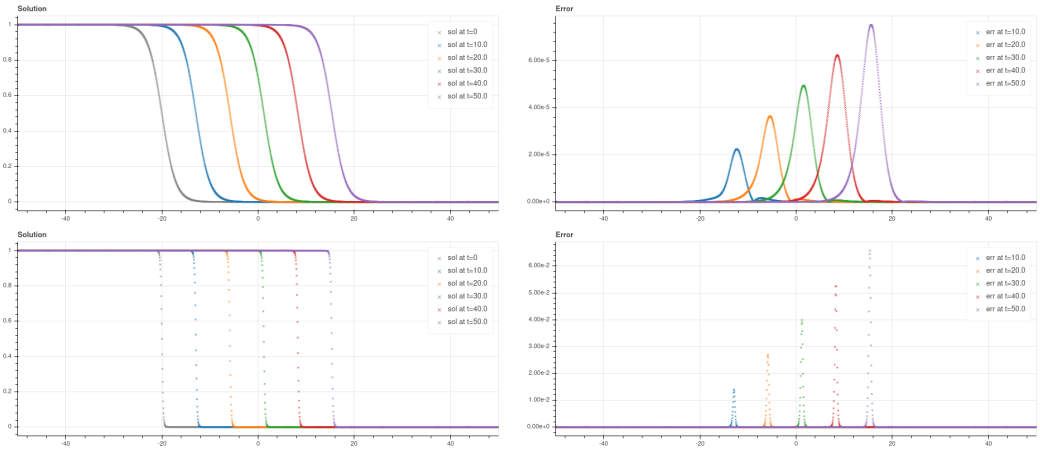

Figure 6: Numerical integration using Radau5 of the system for two couples different (k, D) : $(1.0, 1.0)$ (top), $(10., 0.1)$ (bottom). The bottom one is much stiffer as the gradient is 100 times bigger than the top one. We see that the integration (all parameters being equals except for (k, D)) is much less accurate for the bottom one with an error roughly 1000 times bigger. We also remark that the longer the integration period, the bigger the error. This may be due to an issue with getting the right propagation speed and thus being too slow for example. That would yield to a big error even though the shape of the solution is close to the real one.

0.4.2

To conduct an analysis of the splitting error on $[0, 50]$, we will compare the solution to a quasi-exact numerical solution. Indeed, we have access to a solution on $\mathbb{R}$ however we only look at $[0, 50]$ so it makes more sense to only take the quasi-exact solution. The very fine spatial resolution allows us to only consider time error.

Graph 7 shows the error comparison for several two (k, D) couples : $(1.0, 1.0)$ and $(10, .1)$.

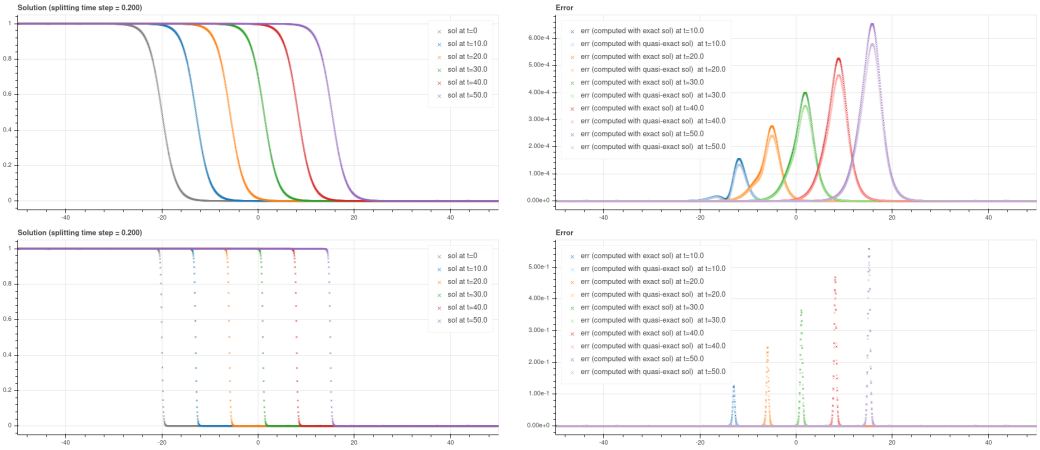

Figure 7: Numerical integration using Strang method of the system for two different couples (k, D) : $(1.0, 1.0)$ (top), $(10., 0.1)$ (bottom). The error is both compared to the real solution and to the quasi-exact one computed using Radau5 with very low tolerance.

0.4.3

The two following paragraphs show how the parameters affect the results, especially the propagation speed and the error that can be linked to a poorly estimated propagation speed.

Wave speed :
The table 1 displays the estimations of the wave speed for two different couples using the Strang splitting method and the quasi-exact Radau5 method.

k	D	Strang	quasi-exact
1	1	0.707037	0.707097
10	0.1	0.699422	0.706353

Table 1: Wave speed values for Strang splitting and quasi-exact solutions for different (k, D) couple values. As expacted, the splitting error increases with the gradient $(\frac{k}{D})^{\frac{1}{2}}$ increasing. We see that the error is roughly 100 times bigger for $(10, 0.1)$ when compared to the quasi-exact solution. Having an error on the wave speed create a phasing between the exact solution and the one obtained with splitting that has for consequence to make the error bigger even though the shape of the solution is the right one. We can also note that in theory, we should have the exact same propagation speed for both cases ($(1, 1)$ and $(10, 0.1)$) which is not the case of the quasi-exact solution where an absolute variation of roughly $7e - 4$ can be observed.

Wave profile :
Graph 8 displays the phase plan for both previous parameter couples.

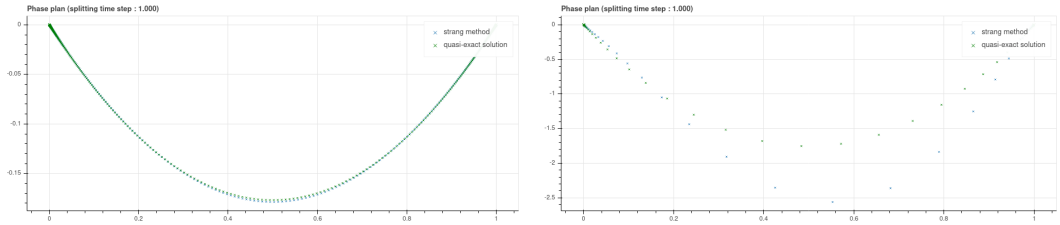

Figure 8: Numerical integration using Strang method (and Radau5 quasi exact solution for comparison) for two different couples (k, D) : $(1.0, 1.0)$ (top), $(10., 0.1)$ (bottom). For the top one, the two remains close which is not the case of the second one. The closer they are, the better the Strang method manages to follow the y-variation of the system.

As we saw in table 1 and graph 8, the bigger $\frac{k}{D}$ is (with $kD = cte$), the bigger the splitting error.

0.4.4

The splitting method strategy for resolving the wave faces one main issue : the difficulty to estimate correctly the propagation speed of the wave, especially for a stiffer system. The Strang method is thus intrasectly unfit

0.5 Simulation of Turing pattern

0.5.1

For $y_{eq} = (a, \frac{b}{a})$, we have : $Df(y_{eq}) = \begin{pmatrix} b-1 & a^2 \\ -b & -a^2 \end{pmatrix}$.

We need the trace to be negative and the determinant positive to have an equilibrium state, meaning :

$$\begin{cases} tr(Df(y_{eq})) & = b - 1 - a^2 < 0 \\ det(Df(y_{eq})) & = a^2 > 0 \end{cases} \tag{2}$$

We thus suppose that : $b - 1 < a^2$ for the rest of the exercice.

0.5.2

Since y_{eq} is an equilibrium, we directly have :

$$\begin{aligned} cos(\frac{n\pi}{L}x)d_t z(t) &= Dz(t)\partial_{xx}(cos(\frac{n\pi}{L}x)) + f(y_{eq} + z(t)cos(\frac{n\pi}{L}x)) \\ &\approx Dz(t)(-(\frac{n\pi}{L})^2 cos(\frac{n\pi}{L}x)) + Df(y_{eq})z(t)cos(\frac{n\pi}{L}x) \text{ (using a Taylor expansion, } f(y_{eq}) = 0) \end{aligned}$$

Which yields :

$$z'(t) \approx z(t)(-D(\frac{n\pi}{L})^2 + Df(y_{eq})) = A_n z(t)$$

with $A_n = -D(\frac{n\pi}{L})^2 + Df(y_{eq})$, which does not depend on x, t.

0.5.3

We have : $A_n = \begin{pmatrix} -d_1 X + b - 1 & a^2 \\ -b & -d_2 X - a^2 \end{pmatrix}$

with $X = (\frac{n\pi}{L})^2$.

Before, we only had stable eigen values. Now we have :

$$\begin{cases} tr(A_n) = b - 1 - a^2 - (d_1 + d_2)X \\ det(A_n) = d_1 d_2 X^2 + (d_1 a^2 - d_2(b-1))X + a^2 \end{cases} \tag{3}$$

The trace is obviously negative by hypothesis (question 1)).

To have unstability of the eigen values we need : $det(A_n) < 0$.

The discriminant of $det(A_n) = d_1 d_2 X^2 + (d_1 a^2 - d_2(b-1))X + a^2$ is : $\Delta = (d_1 a^2 - d_2(b-1))^2 - 4 d_1 d_2 a^2$. To have a possibility for $det(A_n) < 0$, we need $\Delta > 0$ which yields : $(d_1 a^2 - d_2(b-1))^2 > 4 d_1 d_2 a^2$.

$$\begin{cases} (d_1 a^2 - d_2(b-1)) & > 2\sqrt{d_1 d_2}a \textbf{ IF} (d_1 a^2 - d_2(b-1)) \geq 0 \\ & \textbf{OR} \\ -(d_1 a^2 - d_2(b-1)) & > 2\sqrt{d_1 d_2}a \textbf{ ELSE} \end{cases} \tag{4}$$

0.5.4

We take $a = 2$ and $b = 3$ yields : $y_{eq} = (2, 1.5)$. Using $d_2 = 8d_1$, we have : $d_1a^2 - d_2(b-1) = d_1(4 - 8 \times 2) = -12d1 < 0$.

Thus, we need to verify $-(d_1a^2 - d_2(b-1)) > 2\sqrt{d_1d_2}a$: $2\sqrt{d_1d_2}a = 4 \times \sqrt{8}d_1 = 8\sqrt{2}d_1 < 1.5 \times 8d_1 = 12d_1$.

Thus the condition is verified and the equilibrium can be unstable for a wisely choosen X (or (L, n)) verifying :

$$\frac{-(d_1a^2 - d_2(b-1)) - 4d_1}{2d_1d_2} < X < \frac{-(d_1a^2 - d_2(b-1)) + 4d_1}{2d_1d_2}$$

Which yields :

$$\frac{1}{2d_1} < X < \frac{1}{d_1}$$

Which in turn yields :

$$\frac{L}{\pi\sqrt{2d_1}} < n < \frac{L}{\pi\sqrt{d_1}}.$$

0.5.5

For the whole question, the amplitude of the perturbation was choosen as $\epsilon = 0.01$ and $a = 2$, $b = 3$, $d_1 = 1$ and $d_2 = 8$. Our analysis is only valid for ϵ little enough. When it is becomes too big, the non-linear effects take over.

In the following "unstability" means that the solution is not homogeneous but still converge.

First numerical integration : $L = 3$

In this case, to have an unstability, a necessary condition is :

$$\frac{3}{\sqrt{2\pi}} < n < \frac{3}{\sqrt{\pi}}\pi$$

Which corresponds to no $n \in \mathbb{N}$. Thus we observe nothing as displayed on 9.

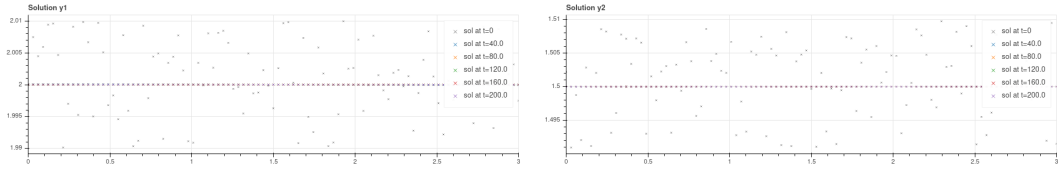

Figure 9: Numerical integration for $L = 3$: y_1 on the left, y_2 on the right.

Second numerical integration : $L = 4$

In this case, to have an unstability, a necessary condition is :

$$1 < \frac{4}{\pi\sqrt{2}} < n < \frac{4}{\pi} > 1$$

Thus $n = 1$ is a unstable harmonic as displayed in graph 11.

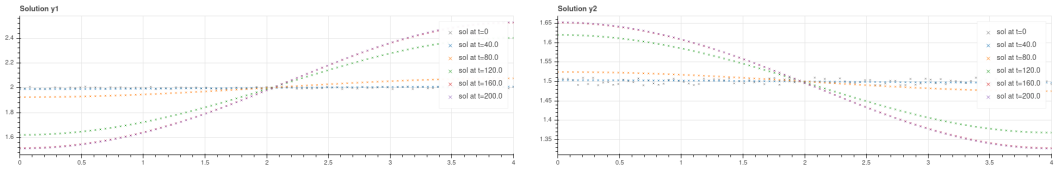

Figure 10: Numerical integration for $L = 4$: y_1 on the left, y_2 on the right. The half period of the periodic harmonic that appears is roughly 4 which is consistent with a $2L$ period and thus with the first harmonic.

Third numerical integration : $L = 7$

In this case, to have an unstability, a necessary condition is :

$$1.57 \approx \frac{7}{\sqrt{2}\pi} < n < \frac{7}{\pi} \approx 2$$

Thus $n = 2$ is an unstable harmonic as displayed in graph 11.

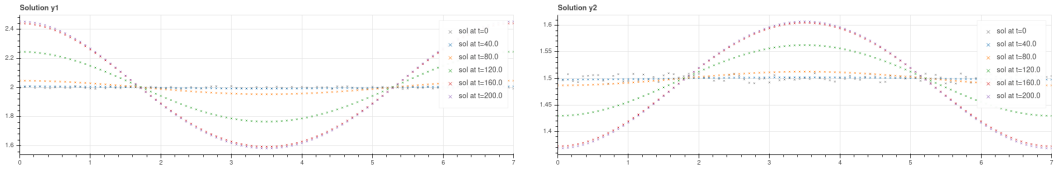

Figure 11: Numerical integration for $L = 7$: y_1 on the left, y_2 on the right. The harmonic that is displayed has this time a period of 7. We find again $\frac{2L}{n} = \frac{14}{2} = 7$

Fourth numerical integration : $L = 20$

In this case, to have an unstability, a necessary condition is :

$$4.5 \approx \frac{20}{\pi\sqrt{2}} < n < \frac{20}{\pi} \approx 6.4$$

Thus $n = 5, 6$ are unstable harmonics. This yields to a periodic signal that has for shorter period (sum of two cosinus: $cos(a) + cos(b) = 2cos(\frac{a+b}{2})sin(\frac{a+b}{2})$) : $\frac{2\times 2L}{n_1+n_2} = \frac{80}{11}$. The longer period as for period : $\frac{2\times 2L}{n_2-n_1} = \frac{80}{1} = 80$. This signal is displayed in graph 11.

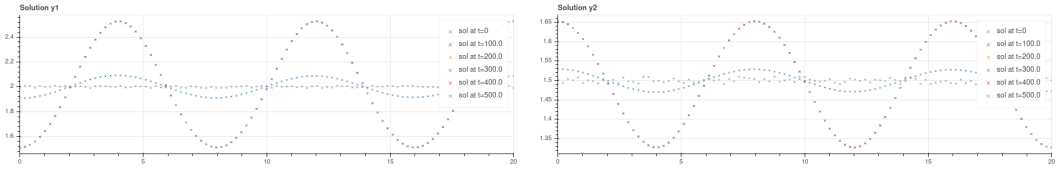

Figure 12: Numerical integration for $L = 20$: y_1 on the left, y_2 on the right.